Contourite drifts as indicators of Cenozoic bottom water intensity in the eastern Agulhas Ridge area, South Atlantic

Jens Gruetzner[1*] and Gabriele Uenzelmann-Neben[1]

1 Alfred-Wegener-Institut, Helmholtz-Zentrum für Polar- und Meeresforschung, Am Alten Hafen 26, D-27568 Bremerhaven, Germany. Jens.Gruetzner@awi.de, Gabriele.Uenzelmann-Neben@awi.de

* Corresponding author

Abstract

High-resolution multichannel seismic reflection profiles acquired in the Agulhas Ridge area (eastern sub-polar South Atlantic) were used in conjunction with multibeam bathymetry and Ocean Drilling Program Leg 177 borehole data to characterise deep water contourite formation in the area of the northeastern Agulhas Ridge and the Cape Rise Seamounts. The transverse ridge separates the Cape Basin from the Agulhas Basin and controls the exchange of water masses between these two basins. Small scale buried drifts, moats and sheet like deposits indicate that sedimentation was controlled by bottom currents since the late Eocene. After a pronounced early Oligocene erosional event resulting from the onset of Lower Circumpolar Deepwater (LCDW) flow, drift formation intensified. The type, position and formation history of the interpreted drifts suggest that the pathways of LCDW flow have undergone little change during the last ~33 Ma and followed roughly todays 4900 m depth contour. Northwest of the Cape Rise Seamount we found a mounded drift with an oval shape, a height of ~400 m and a width of ~50-60 km indicating a clockwise circulating bottom water gyre in that area. Extensive drifts in the Cape Basin occur as features confined between the Agulhas Ridge and Cape Rise seamounts and as mounded and sheeted drifts further to the West. The confined drifts show erosional features on both flanks suggesting a West setting bottom water flow along the northern flank of he Agulhas Ridge and an opposing eastward directed flow along the southern rim oft he Cape rise seamount group. In contrast to the large drift deposits in the Cape Basin smaller, confined drifts showing more erosional features are found south of the Agulhas Ridge. Together these findings suggest that the deepest LCDW flowed anticlockwise around the Agulhas Ridge before taking a major clockwise loop in the Cape Basin. The returning bottom water then flowed around the Cape Rise seamounts before entering the Indian Ocean.

Key words: Contourites; bottom current; South Atlantic; Agulhas Ridge; Paleoceanography; seismic-reflection data

1. Introduction

Seismic investigations of contourite drift deposits have been extensively used to unravel the Cenozoic evolution of deep ocean circulation (Rebesco et al., 2014). The location, shape and internal structure of the sediment drifts can be used as indicators of changing pathways and intensities of bottom currents (Rebesco and Camerlenghi, 2008). This approach has been particularly successful on continental margins where deep western boundary currents created large contourite depositional systems (Hernández-Molina et al., 2008a; Muñoz et al., 2012; Nelson et al., 1999). However, far less is known about the history of bottom currents in the deep ocean basins and abyssal plains. In many cases, current controlled sedimentation in basinal systems is accompanied by the deposition of large sheeted drifts with a low-mounded geometry (Carter and McCave, 1994; Escutia et al., 2002; Maldonado et al., 2005; Masson et al., 2002). These drifts drape the pre-existing morphology of the oceanic basement and were formed by the current action of tabular water masses (Hernández-Molina et al., 2008b). In parallel, topographic features within or at the rim ocean basins such as seamounts ridges and plateaus can disrupt and accelerate the flow and also influence the current pathway (e.g. Merrifield et al., 2001). These changes are often leading to the formation of moats and mounded sediment drifts (Hernández-Molina et al., 2008b; Maldonado et al., 2005; Masson et al., 2003; Müller-Michaelis et al., 2013). A spectacular example of such topographic obstacles for deep ocean currents in the south Atlantic is the Agulhas Ridge, which forms an elongated part of the Agulhas-Falkland Fracture Zone (AFFZ) rising ~3,000 m above the surrounding seafloor (Fig. 1). Constituting an important topographic barrier, the ridge has a strong influence on the exchange of water masses between high and lower latitudes (Fig. 1).

Geochemical proxies (such as $\delta^{13}C$ or ε_{Nd}) measured on samples from sediments drilled on the Agulhas Ridge (Hodell et al., 2002) have helped to decipher Cenozoic variations of water masses related to climate changes in the South Atlantic (Billups et al., 2002; Scher and Martin, 2008). Variations of neodymium isotope ratios on the Agulhas Ridge (ODP Site 1090) suggest an influx of shallow Pacific seawater to the South Atlantic sector oft he Southern Ocean at approximately 41 Ma that may indicate an early opening of the Drake Passage (Scher and Martin, 2006). Information on how these changes in transport influenced the intensity and position of current systems is currently sparse. They can, however, be gained by seismic investigations of contourites (Wildeboer Schut et al., 2002).

Here we present new multichannel seismic profiles recorded in the hitherto unexplored area of the Northeast Agulhas Ridge (Fig. 1b) that complement earlier data. A reconnaissance survey in the area of the western Agulhas Ridge provided evidence for sediment drift formation on both sides of the ridge due to a bottom current flow that intensified at the Eocene/Oligocene boundary (Uenzelmann-Neben et al., 2007; Wildeboer Schut and Uenzelmann-Neben, 2005; Wildeboer Schut et al., 2002). We combine our seismic interpretation with new bathymetric data from a multibeam survey and geological information from Leg 177 of the Ocean Drilling Program (ODP) which recovered high-quality sedimentary sequences at seven sites between 41° and 53°S for studying the Cenozoic history of the high-latitude South Atlantic Ocean(Hodell et al., 2002). Three of these ODP Leg 177 sites (1088, 1089, 1090) are located on the Agulhas Ridge (Hodell et al., 2002) and especially data from Site 1090 is used here for integrating geological and seismic information.

The study investigates the evolution of newly discovered sediment drifts in deep (> 4000 m) water and major oceanographic changes governing their formation. In particular we infer changes in bottom current intensity as well as temporal and spacial variations in the position of these currents.

2. Geologic setting and hydrography

The Agulhas Ridge comprises a ~ 650 km long feature of the Agulhas-Falkland Fracture Zone which developed as part of the break-up of Gondwana in the early Cretaceous (Ben-Avraham et al., 1997) (Fig. 1). The ridge is of tectono-magmatic origin (Hartnady and Leroex, 1985) and it rises almost 3000 m above the surrounding seafloor. This bathymetric anomaly is likely related to a jump in spreading axis at ~83 Ma (chron C34) which placed the spreading axis further west in the Agulhas Basin and/or with the paleo-position of the Shona mantle plume during the early opening of the South Atlantic Ocean (le Roex et al., 2010).

The southwestern part of the ridge is characterized by up to four parallel segments separated by deep depressions, which are filled with up to 1s TWT of sediments (Wildeboer Schut and Uenzelmann-Neben, 2005). Here the ridge shows only a thin sedimentary cover. In contrast, the northeastern Ridge forms a 110 x 185 km wide plateau which is covered with > 1000m of sediment. Basement structures controlling the distribution of the sedimentary units reflect a tectono-magmatic reactivation in Oligocene times or younger (Uenzelmann-Neben and Gohl, 2004) . The origin of the reactivation is suspected to be material channelled from the Discovery Hotspot west of the Agulhas Ridge. The Cape Rise seamounts including the large Schmitt-Ott seamount are located ~100 km northwest of the eastern Agulhas Ridge (Fig. 1b). Similar to the Agulhas Ridge they have been argued to represent the surface expressions of mantle plumes (le Roex et al., 2010).

The Agulhas Ridge is located in the northern Subantarctic Zone between the Subtropical Front (STF) and the Subantarctic Front (SAF) to the south. The water depth over the ridge shoals from ~4900 m to ~1900 m and thus the topographic feature intersects all major deep- and bottom-water masses in the Southern Ocean (Fig. 2), having a strong influence on the exchange of these water masses between high and lower latitudes. The deepest water mass in subpolar Southern Ocean is the Lower Circumpolar Deep Water (LCDW), which comprises a mixture of Antarctic Bottom Water (AABW) and deep-water masses from all ocean basins supplied by the Antartic Circumpolar Current (ACC). CDW enters the southeast Atlantic basins through deep fracture zones in the Mid-Ocean Ridge. Its northward spreading is blocked by the Agulhas Ridge which directs the CDW route towards the West and the East (Fig. 1). Thus, much of the CDW enters the Cape Basin as a bottom current through a passage between South Africa and the north-eastern tip of the Agulhas Ridge (Tucholke and Embley, 1984). The bottom flow is then guided south westward by the topographic elevation of the Agulhas Ridge and follows a clockwise pathway through the Cape Basin (Fig. 1).

Furthermore the Agulhas Ridge is located within the modern mixing zone of CDW and North Atlantic Deep Water (NADW). In the southeast Atlantic, the NADW core is splitting the CDW into an upper (UCDW) and lower (LCDW) flow and can be identified by its physical and chemical composition (Pena and Goldstein, 2014). For example it has a higher salinity (S = ~34.8 psu) and a less radiogenic neodymium isotopic composition (ε_{Nd} = ~–10.5) as present-day UCDW and LCDW (S = 34.6 – 34.7 psu, ε_{Nd} = ~9.5 – 10.0, Fig. 2)(Stichel et al., 2012). As such, major changes in the mean water-mass composition of the deep ocean are reflected in geochemical proxies measured on sediments cored or drilled in the area (Anderson and Delaney, 2005; Billups et al., 2002; Charles and Fairbanks, 1992; Scher and Martin, 2006). The NADW pathway into the Cape Basin is a zonal flow across the interior at 25°S carrying NADW eastward (van Sebille et al., 2012). Then NADW flows southward along the western edge of the African continent within a broad slope current, continuing around the tip of South Africa to exit the Atlantic basin beneath the Agulhas Current System (Arhan et al., 2003). Antarctic Intermediate Water (AAIW) originates from surface water around Antarctica, flows northwards into the South Atlantic and extends to water depths of 1000 m (Fig. 2). In the Cape Basin AAIW follows an anticyclonic path (Shannon and Hunter, 1988), opposite to the direction of the underlying UCDW.

At the surface, the Agulhas leakage is the main source of warm and salty waters carried towards the Subpolar North Atlantic as the upper limb of the Meridional Overturning Circulation (Biastoch et al., 2008). The kinetic energy of individual Agulhas rings may reach down to 3000 m water depth (Dencausse et al., 2010) and influence the pathway of deep-water masses (van Sebille et al., 2012).

3. Data and Methods

RV Maria S. Merian cruise MSM 19/2 undertaken in 2011 comprised geophysical operations in the area of the Agulhas Ridge (Uenzelmann-Neben, 2012). Reflection seismics as well as PARASOUND and multibeam systems were used in order to study the sedimentary distribution in relation to the tectonic and oceanographic evolution of the area (see yellow lines in Fig. 1). Profiles with a total length of 5400 km cover the whole Agulhas Ridge, the transition into the deep sea and also cross the locations of ODP Leg 177 Sites 1088, 1089, and 1090(Gersonde et al., 1999) (Fig. 1a). The new seismic profiles were jointly interpreted with available seismic data from a reconnaissance survey (Wildeboer Schut et al., 2002) resulting in a seismic network of more than 3800 km in the investigated area.

The high-resolution seismic reflection data were collected in the northeastern part of the Agulhas Ridge and in the area of the Cape Rise seamounts. Four air-guns, with a volume of 1.4 l each, were used as a seismic source. Each of the guns consisted of a generator chamber (0.72 l volume), and an injector chamber (1.68 l volume), triggered with a 33 ms delay to suppress any bubble effect. The guns were towed 30 m behind the vessel in 2 m depth and seismic shots were generated every 10 s at a constant ship speed of 5 knots, resulting in a shot-spacing of approximately 25 m. The recording system consisted of a 3000 m long streamer with 240 channel hydrophon array. Data with a sample interval of 1 ms and a recording time of 9 s were received using a high-resolution seismic data acquisition system (SERCEL SEAL©). Ship's GPS (Global Positioning System) navigation data were used for geometry definition and common depth point (CDP) sorting with a CDP spacing of 25 m. Further processing of the seismic reflection data consisted of precise velocity analysis (every 50 CDP), normal moveout correction, stacking, and time-migration (Omega-X migration). Band-pass filtering with tapering (Hanning window) with the boundaries between 20–25 Hz and 200–250 Hz was applied to the displayed data. Since seismic amplitude information was used for the interpretation we avoided AGC (Automatic Gain Control) filtering.

Bathymetric data were recorded parallel to the seismic profiling. Swath bathymetric mapping was conducted throughout the cruise MSM19/2 with the echo sounder system SIMRAD EM120 (12 kHz). During the cruise the angular coverage sector was adjusted according to the weather conditions and data quality. It varied between 130° during regular sea conditions and 100° during rougher weather conditions when a high noise level was observed in the acquired data (Uenzelmann-Neben, 2012).

Large-scale density currents are generally in geostrophic balance and flow parallel to the isobaths (Wåhlin and Cenedese, 2006). We here derive bottom flow direction from the position of mounded contourite drift deposits and erosional features under the prerequisite that in the southern hemisphere Coriolis forces deflect bottom currents towards the left, focus the flow vortex against the adjacent seafloor of the slope, and erode the left flank of the drift, whereas slower flow and deposition takes place on the right flank (Faugères et al., 1999). In addition the occurence sheeted drifts point towards deposition under a broader tabular flow regime (Hernández-Molina et al., 2008b; Masson et al., 2002; Stow et al., 2002).

Indications on the relative intensities of bottom currents are inferred from the type and geometry of the contourite ridges, which in the working area consist mainly of mud and ooze (Shipboard Scientific Party, 1999). In such fine-grained drifts, sediment can accumulate under flow velocities of 5-20 cm/s (McCave and Hall, 2006; Stow et al., 2009). Higher flow velocities (>30 cm/s) are generally associated with erosional structures like moats and contourite channels cutting into the seafloor at the rim of the drifts. On continental slopes unconformities within contourite drifts are often diachronic and can interfinger with correlative hiatuses or aggraded strata in axial regions of contourite drifts (Alves, 2010). Mudwaves can hardly form when the flow velocity exceeds 17 cm/s (Flood, 1988). Also internal reflector strength has been used as a qualitative estimate for current strength (Müller-Michaelis et al., 2013), although an unequivocal correlation between sediment facies and seimic attributes does yet not exist (Nielsen et al., 2008). While homogenous acoustically transparent units may point towards stable moderate flow speeds, high amplitude reflector sequences can indicate large temporary changes in current strength or sediment supply (Nielsen et al., 2008).

4. Results

4.1 Seismic stratigraphy

A suite of seismic reflectors traced in the southwestern Agulhas ridge area was dated based on correlation with ODP Sites 1088, 1089 and 1090 via synthetic seismograms (Wildeboer Schut and Uenzelmann-Neben, 2006). Based on these marker horizons, the internal reflector strength and the overall geometry we here define 3 main seismic units (SU1 – SU3) in the working area (Figs. 3 and 4).

SU1 comprises a homogenous semi-transparent package with a maximum thickness of ~0.3 s TWT that fills and drapes the acoustic basement. This transparent interval is topped by a series of 3-4 high amplitude reflectors and a second thinner (~0.1 s TWT) transparent package (Fig. 4). At ODP Site 1090 only the topmost part of SU1 was reached and revealed middle Eocene carbonate rich sediments (Shipboard Scientific Party, 1999). The boundary between SU1 and SU2 is marked by the lowermost of the high amplitude reflectors, which we use as stratigraphic marker horizon E for the middle Eocene (~39 Ma). Reflector E is caused by drastic change in sediment physical properties (e.g. a downward density increase from 1.6 to 1.8 g/cm^2) occurring at ~340-350 m at ODP Site 1090 (Fig. 3) which is caused by change in lithology from diatomaceous muds to nannofossil oozes and chalks.

SU2 is formed by a 0.1 to 0.2 s thick interval of high amplitude reflections that are present throughout the basin (Fig. 4). Drill cores from Site 1090 show that this middle Eocene to lowermost Oligocene (38.9 and 33.4 Ma) interval (Diekmann et al., 2004) consists of an extended succession (118 m thickness) of grey diatomaceous oozes and muds with occasional calcareous layers (Fig. 3). The top of SU2 is formed by the prominent stratigraphic marker horizon O which represents a pronounced unconformity and can easily be identified also in the northeast Agulhas ridge area (Figs. 3 and 4). At ODP Site 1090 the unconformity O appears as a 1.5-Ma hiatus around 32 Ma (Diekmann et al., 2004). A change from the predominently diatomaceous lithology of Unit 2 towards overlying oozes and muds at 220 m depth (Gersonde et al., 1999) results an abrupt increase in acoustic impedance which produces the seismic reflector O (Wildeboer Schut and Uenzelmann-Neben, 2006). A similar early Oligocene unconformity is found in several drilling locations in the area, e.g. at ODP Site 703 on the Meteor Rise (Hailwood and Clement, 1991).

SU3 is highly heterogeneous in the working area and reveals a considerable topography due to the presence of mounded and elongated drifts, as well as depressions like moats and channels. Further features shaping the seafloor towards the top of unit 3 are sediment sheets and mudwaves (Fig. 4d, CDPs 2300 – 2900). Overall a relief ranging from a few meters to several hundreds of metres has been built up in the working area (Fig. 4) and further towards the Southwest (Wildeboer Schut and Uenzelmann-Neben, 2005). In some profiles SU1 has a semi-transparent appearance directly above the early Oligocene unconformity O (Fig. 4a), but the reflection strength gradually increases upwards. In the areas where SU3 is thicker, it can be further subdivided by the dated reflectors M (middle Miocene) and P (early Pleistocene) (Figs. 3 and 4d). However, these horizons are difficult to identify Northwest of the Agulhas Ridge and around the Cape Rise seamounts.

4.2 Contourites in the Cape basin

In the Cape Basin the working area comprises two areas where previously unknown bottom current related sediment structures were found: The passage between the Agulhas Ridge and Cape Rise Seamounts (Figs. 1, 4 and 5) and the area west of the Cape Rise Seamounts (Fig. 6).

At the northeastern entrance of the passage between the Agulhas Ridge and the Cape Rise seamounts a mounded sediment drift is located (Fig. 4a, CDPs 5500 – 8600). The drift mound has a height of ~ 300 m above its base at reflector O. Sub-parallel, high-amplitude reflectors pinching out at the seafloor on both flanks of the mounded structure alternate with transparent intervals. The base of the drift formed by reflector O inclines towards the Northwest where it cuts into the high amplitude reflectors of SU2. A buried moat is visible between CDPs 5800 and 6200 in profile 20110418 (Fig. 4a). The mounded drift is covering the seafloor and thus can be identified in the shipboard bathymetry but the drift can also be followed roughly in the 30 arc-second global grid of elevations (GEBCO 2014) (grayshades in Fig. 5). The width oft the drift is ~80 – 100 km km in the Northeast of the working area and its elongated crest is striking SW – NE. Towards the Southwest the drift is increasingly confined by the passage between the ridge and the seamounts.

The narrowest deepwater passage between the Agulhas Ridge and the Schmitt-Ott seamount is displayed in profile 20110416. Here, a sediment drift is plastered onto the volcanic apron of the Schmitt-Ott seamount (Fig. 3b, CDPs 4000 – 5100). A 150 m deep and 10 km wide erosional channel (Fig. 4b, CDPs 5100 – 5500) is separating the drift from the Agulhas Ridge. Erosion in the channel reached down to reflector O that forms the base of the drift body towards the Northwest.

In the area directly adjacent to the southwest of the narrow passage, SU3 exhibits a thin sedimentary column (~140 ms, ~130 m) that is low mounded at the position of profile 20110415 (Fig. 2, CDPs 5300 – 6500) and sheeted further towards the Southwest (Fig. 4c). Both profiles reveal moats at the northwestern rim of the Agulhas Ridge. Furthermore, Profile 20110415 exhibits a broad erosional zone on the seafloor adjacent to the Cape Rise seamount (Fig. 2, CDPs 6500 – 7400).

Further towards the southwestern part of the working area where profiles 1998004, -005 (Fig. 4d) and -008 cover an elongated mounded drift investigated by Wildeboer Schut et al. (2002). Here SU3 reaches a maximum thickness of ~500-600 m and shows variable topography. Interesting features are two drift crests at CDPs 700 and 1800 (Fig. 4d) respectively that show opposing trends of migration towards the center of the elongated drift. Another crest at CDP 200 (Fig. 4d) is also inclined towards the Southeast but may have been affected by faulting (Fig 4d, CDP 600). Irregular mudwaves occur at the southeastern edge of the elongated drift (Fig. 4d, CDPs 2800 – 3000).

West of the Cape rise seamounts seismic profiles 20110415, -16, -22 and -23 and bathymetric data reveal a mounded sediment drift (Fig. 6). The structure has a rounded, slightly oval (45 x 65 km) shape that displays a shallower relief in the North but increasing topography (max. 450 m above reflector O) towards the South (Fig. 6d). The southeastern rim of the structure is separated from the Schmitt-Ott Seamount by a moat (e.g. Fig. 6c, CDPs 2000 – 2400). Reflector sequences inside the drift body are convex upward. Evidence for strong erosion is also found towards the west (Fig. 6b, CDPs 6200 – 7100) of the drift. The base of the drift is formed by reflector O.

4.3 Contourites in the Agulhas Basin

Seismic profile AWI-20110419 (Fig. 7) shows a number of small scale (5 – 10 km wide, 100 – 150 m high) mounded drift bodies typical for the southern rim of the Agulhas Ridge located in the Agulhas Basin. Individual drifts are confined between basement highs and are separated by moats. Reflector strength inside the drifts is often increasing upward. However, some drifts show an intercalation of semitransparent and high-amplitude intervals (Fig. 6, CDPs 6800). It is not possible to correlate these deposits with the stratigraphic information from drillsites and therefore their formation history cannot be resolved in detail. The drift closest to the Agulhas Ridge has been deposited on top of a sediment package that fills a basement trough and is characterized by parallel high amplitude reflectors (Fig. 7, CDPs 4800-5400).

5. Discussion

5.1 Indications for Pre-Oligocene deep water circulation

Pre middle Eocene (> 39 Ma, below reflector E) sediment deposits (SU1) at the Agulhas Ridge appear as a drape and fill of the acoustic basement with the internal reflector geometry reflecting basement topography. The sheet-like, acoustically transparent sediment cover indicates deposition by pelagic settling through the water column and/or current action under a tabular flow with very low flow speeds. A pelagic depositional environment is also indicated by the lowermost sediments drilled at ODP Site 1090 (Fig. 3) that represent the top of SU1 and consist of red clay bearing nannofossil oozes of middle Eocene age which were deposited at sedimentation rates of < 20 m/m.y. (Shipboard Scientific Party, 1999). Intervals of higher reflector strength within SU1 may be due to the deposition of turbidites or the formation of cherts (Diekmann et al., 2004).

SU2 represents the time interval from the middle Eocene to the lowermost Oligocene, consists of a series of high amplitude reflections, and exhibits in some places small-scale buried drift structures and buried moats. In the working area these contouritic structures occur at the rim of an elongated mounded drift between the Agulhas Ridge and the Cape Rise Seamounts (e.g. Fig. 4a, CDPs 5800 – 6400) and are thus coeval to buried contourites found further towards the Southwest (Wildeboer Schut and Uenzelmann-Neben, 2005). Compared to similar contouritic features deposited later on, the older buried structures are of a much smaller scale (Fig. 4a) and are not visible northwest of the Cape Rise seamounts. This may point towards limited current control on sedimentation during the middle Eocene/early Oligocene (~39 – 33 Ma). However, considering that the sediments displaying the high amplitude sheet like reflector sequences were deposited contemporaneously with the buried drifts and that the sedimentation rates were high (> 30 m/m.y) during that interval we can classify the majority of SU2 deposits as sheeted drift deposits. Larger Eocene mounded sediment drifts were possibly in existence but may have been eroded away by the strong erosional forces associated with unconformity O. At ODP Site 1090 higher silt concentrations in the late Eocene/early Oligocene sediments compared to the very fine-grained middle Eocene section may indicate an increase in current control on sedimentation. The gradual increase of the silt fraction occurred between ~41 and 38 Ma and was followed by an opal pulse indicating increased phytoplankton production and stronger upwelling (Diekmann et al., 2004). Thus, SU2 here is interpreted as bottom current controlled with the series of high amplitude reflections possibly caused by climate related changes in biogenic opal production.

The timing of this current influenced sedimentation regime is in agreement with buried drift structures that were recently found in the area east of New Zealand (sub-polar South Pacific) (Horn and Uenzelmann-Neben, 2015) and related to a Proto-Deep Western Boundary Current (Proto-DWBC). The formation of such a Proto-DWBC that developed along with the middle/late Eocene global cooling trend (Zachos et al., 2001) is supported by a numerical simulation (Sijp et al., 2011) and may have been caused by enhanced cold deep water (Proto- AABW) production due to East Antarctic glaciations (Ehrmann and Mackensen, 1992).

The evidence from the Agulhas Ridge for middle/late Eocene bottom currents suggests that the Proto-AABW took a north setting path also into the South Atlantic and that deep water formation took place around a large but possibly ephemeral (Zachos et al., 2001) pre-Oligocene East Antarctic Ice Sheet. Furthermore secular variations of neodymium isotope ratios (Scher and Martin, 2006) at the Agulhas Ridge suggest a middle Eocene influx of shallow Pacific seawater into the South Atlantic and thus may indicate the existence of a Proto-Antarctic Circumpolar Current (Proto-ACC) at that time. Although the Tasmanian Gateway was still closed during the late Eocene (Barker et al., 2007) the conditions for a (weaker then today) proto-ACC were likely met (Bijl et al., 2013; Eagles et al., 2006; Munday et al., 2015).

5.2 Early Oligocene to present day LCDW circulation in deep-water basins

The erosional unconformity represented by reflector O marks a time interval around 33 Ma when a considerable amount of sediment was removed from the Agulhas Ridge area due to very strong current activity. This event occurred contemporaneously with a major global increase in benthic oxygen isotopes due to the formation of a large East Antarctic ice sheet and deep-water cooling (Zachos et al., 2001). The onset of vigorous bottom current circulation led to the development of prominent unconformities that can be found in the western South Atlantic (Gruetzner et al., 2012; Hernández-Molina et al., 2009; Hinz et al., 1999), the southern Indian Ocean (Niemi et al., 2000; Uenzelmann-Neben, 2001), and the South Pacific (Carter et al., 1994; Horn and Uenzelmann-Neben, 2015). The event is also documented by a hiatus at several drilling locations (Carter et al., 2004; Gersonde et al., 1999; Hailwood and Clement, 1991; Tucholke and Embley, 1984). At ODP Site 1090 the hiatus is identified for the time span between 32.8 and 31.3 Ma (Marino and Flores, 2002) and is accompanied by a drop in sedimentation rates and a lithologic change from diatomaceous oozes and muds below O to pale grey calcareous oozes and muds (Gersonde et al., 1999) above (Fig. 3). This change from biosiliceous to carbonate sedimentation may be related to shifts of oceanic fronts possibly caused by Pacific water that was entrained in the LCDW and transported to the Agulhas Ridge from ~33 Ma onward as indicated by Neodymium isotopes (Scher and Martin, 2008) and major element ratios (Latimer and

Filippelli, 2002).

Subsequently mounded sediment drifts formed on top of horizon O indicating that bottom current flow slowed down into the range (< 20 cm/s) in which the formation of such features is feasible (McCave and Hall, 2006; Stow et al., 2009). The lithology of SU3 at Site 1090 reveals variations in the input of terrigenous and biogenic matter (Fig. 3a) and is generally fine-grained. These sediments are mostly bioturbated but in some intervals show laminations (Shipboard Scientific Party, 1999) which is typical for muddy contourites (Rebesco et al., 2014; Stow and Faugères, 2008). The inferred flow speed reduction may have been related to the full development of the ACC at 30 Ma (Scher et al., 2015) which coincides with stronger Atlantic Meridional Ocean Circulation (AMOC) and a shift towards the modern four-layer ocean structure (Katz et al., 2011). The core flow with highest flow intensities occurred in channels and moats along the rim of the volcanic basement topography present in the area. Geochemical proxies provide evidence that LCDW as a mixture of AABW and other water masses is forming since the early Oligocene (Latimer and Filippelli, 2002; Scher and Martin, 2008) and from the stability of the sediment drifts we conclude that the LCDW flow path has undergone little change since its establishment. This flow path of bottom water through the Agulhas ridge area is derived in detail using the position and shape of the contourites (Fig. 8):

Along the southern flank of the ridge small patchy drifts formed in the Agulhas basin. The formation of numerous small drift bodies and moats between the basement highs (Fig. 7) indicate that bottom current flow in the Agulhas Basin took place in complex patterns around the volcanic obstacles. However, from a series of elongated mounded drifts that were deposited along the Agulhas Ridge we conclude that the main flow was east setting along the ridge (Fig. 8). It is not possible to directly tie the lithologic and age information from any of the Leg 177 drill sites. The reduced height of the drift bodies likely indicates that on average the flow was quite vigorous. Coriolis force deflects the flow towards the left and currents were guided around the northeastern corner of the Ridge into the Cape basin.

At the northeastern entrance of the passage between the Agulhas Ridge and the Cape Rise seamounts the inclination of reflector O towards the seamounts indicates that the vigorous bottom water flow in the early Oligocene was even higher in the northern part of the gateway (Fig. 4a). Subsequently a mounded sediment drift grew over the inclined (Fig. 4a, CDPs 5500 – 8600) surface O pointing towards a reduction in flow speed. The core flow with highest intensity thus migrated towards the Southeast. However, strong erosional forces commenced on both sides of the feature (Fig. 4a) as indicated by reflectors pinching out on both flanks of the drift. Together seismic profiles and bathymetric data reveal that the drift is covering at least (the northeastern extend is unknown) 3800 km^2 of the seafloor (Fig. 5) and can be classified as a mounded confined drift (Faugères and Stow, 2008). Towards the Southwest the deep basement trough between the ridge and the Schmitt-Ott seamount narrows to ~25 km (Fig. 4b) and forms the southwest termination of the confined drift. Here the main deep and vigorous flow was confined to the 10 km wide channel at the base of the Agulhas Ridge.

Southwest of this narrow passage a deeply eroded SU1 observed in profiles 20110415 and -20 (Figs. 2, 4c) suggests that here bottom water flow was strong over the full width of the gateway. Presumably this is an area where the interaction of the southwest setting current along the Agulhas Ridge and a northeast directed flow around the Cape Rise seamounts (see below) caused a higher vorticity (Fig. 8). The south-westbound flow was then channelized again towards the ridge and created a larger (> 15000 km^2) elongated, mounded drift on top of erosional surface O that extends ridge-parallel to at least 9°E

(Wildeboer Schut and Uenzelmann-Neben, 2005).

Directly northwest of the Schmitt-Ott seamount a mounded sediment drift covering an area of ~1200 km^2 is located on top of unconformity O and thus appears to have been formed contemporaneously with the extensive current controlled deposits north of the Agulhas Ridge (Fig. 4a). The rounded (oval) form and the fact that the drift mound is facing the seamount, separated by a moat points towards a stable bottom current flow along the edge of the seamount. Under the premise of a leftward Coriolis related current deflection in the Southern hemisphere we can infer clockwise circulating bottom water north of the Cape Rise Seamounts (Fig. 6) that is fed by a current from the North. Today the bottom water coming from the North in the Cape Basin is LCDW (Figs. 1 and 2) that takes a clockwise loop in the basin (Arhan et al., 2003; Tucholke and Embley, 1984). There occur extensive erosional features on the slope between the Agulhas Ridge and the African continent (Tucholke and Embley, 1984) likely resulting from bottom water flow on a direct path around the tip of Africa into the Natal Valley. However these features are restricted to shallower (< 4500 m) depth and present bathymetry (Becker et al., 2009) shows no direct conduit for deeper (> 4700 m) waters. Thus the rounded drift at the Schmitt-Ott seamount indicates that the deepest flow (~ 4800-4900 m) of this water mass is likely directed towards the West by the Cape rise seamounts before Coriolis force deflects the current again towards the East in direction towards the Natal Valley (Indian Ocean) (Fig. 8).

6. Conclusions

With the present investigation of new seismic and bathymetric data from the Agulhas

Ridge area we aimed at a better understanding of both pathways and intensity of the current system in the eastern sub-polar South Atlantic. Our results indicate:

1. The seafloor in the Agulhas Ridge and Cape rise seamounts area is covered with current derived sediment deposits and erosional features that have developed since the Early Oligocene on top of a prominent erosional unconformity. In addition to previously known sheeted and mounded sediment drifts we described newly discovered mounded drift deposits NW of the Schmitt-Ott seamount and in the area between the Cape rise seamounts and the Agulhas Ridge that can be classified as confined drifts.
2. The inferred changes in bottom current activity at the Agulhas Ridge from slower tabular flow during the middle and late Eocene (~39 – 33 Ma), over very vigorous current action evidenced by reflector O, towards strong and stable flow (~ 33 – present) are in agreement with a two step development of the ACC suggest by geochemical proxies.
3. Based on the distribution and internal seismic character of erosional and depositional features we derived bottom current pathways and intensities. Overall a complex circulation pattern that is guided by the topography of the volcanic bodies in the area can be inferred. We suggest that the LCDW bottom water flow that takes a clockwise loop in the Cape Basin and roughly follows todays 4900 m depth contour is deflected westward by the Cape Rise seamounts before taking an eastward path into the Indian Ocean.

Acknowledgements

We acknowledge the work of Captain Friedrich von Staa, his officers and crew of RV Maria S. Merian cruise MSM 19/2. We like to thank also the technicians and scientific staff of RV for their support during the measurement programme. The ship time of RV Maria S. Merian was provided by the Deutsche Forschungsgemeinschaft within the core program METEOR/MERIAN. We also benefited from financial contributions by the research institutes involved. We are grateful to Tiago M. Alves and an anonymous reviewer for their detailed and helpful comments.

Figures

Figure 1. (a) Bathymetric map with the general circulation scheme of deep-water masses south of Africa (Tucholke and Embley, 1984; Uenzelmann-Neben et al., 2007). (LCDW = Lower Circumpolar Deep Water; AAIW = Antarctic Intermediate Water; NADW = North Atlantic Deep Water) and locations of reflection seismic profiles shot in 1998 (black lines) and 2011 (yellow lines). Stars indicate the positions of ODP Leg 177 drill sites. Orange box indicates working area shown in Figs. 1b and 7a. (b) Detailed location of seismic profiles over the eastern Agulhas Ridge. Intervals shown in figures are marked by thicker lines.

Figure 2. Reflection seismic profile AWI-20110415 in combination with a meridional hydrographic profile in the present-day South Atlantic showing the different water masses

(LCDW = Lower Circumpolar Deepwater, NADW = North Atlantic Deep Water, UCDW = Upper Circumpolar Deepwater, AAIW = Antarctic Intermediate Water) based on the salinity distribution (colour coded)(World Ocean Atlas) in relation to seafloor morphology and the sub-bottom sediment geometry. White isolines correspond to the modern South Atlantic seawater Neodymium isotope ε_{Nd} composition (Pena and Goldstein, 2014; Stichel et al., 2012). Circles indicate the inferred bottom current directions. Red line marks reflector O (early Oligocene). VE = Vertical exaggeration.

Figure 3. Sedimentary log (a) of ODP Site 1090 tying the interpreted horizons E, O, M, and P to stratigraphic, bulk density (b), and synthetic seismic data (c) (modified after (Wildeboer Schut and Uenzelmann-Neben, 2006)).

Figure 4. Sediment drift deposits between the Agulhas Ridge and the Cape Rise Seamounts as displayed in seismic reflection profiles. Reflectors E (middle Eocene), O (early Oligocene), M (middle Miocene), P (Pleistocene) are marked in cyan, red, green and orange, respectively. Seismic units (SU1-3) are indicated. See Figures 1b and 5 for location of the lines. Vertical exaggeration is ~30 in all profiles.

Figure 5. Bathymetric chart showing the outline (thick yellow line) of an elongated mounded sediment drift between the Agulhas Ridge and the Cape Rise Seamounts. Shipboard multibeam bathymetry (colour coded) is overlain over global (GEBCO) bathymetry grid (greyscale). Seismic profiles shown in Figs. 2, 4a and 4b are marked by orange lines. Thin yellow lines are other interpreted seismic lines (not shown). Black numbers are CDPs. White arrows indicate the inferred flow paths of LCDW.

Figure 6. (a-c) Mounded oval sediment drift northwestward of the Schmitt-Ott Seamount (Cape Rise Seamounts) as seen in seismic profiles. Circles indicate the inferred bottom current directions. Red line marks reflector O (early Oligocene). (d) Shipboard multibeam bathymetry (colour coded) overlain over global (GEBCO) bathymetry grid (greyscale). Profiles shown in a-c and Fig. 2 are marked by orange lines. Black numbers are CDPs. A thick yellow line outlines the sediment drift. White arrows indicate the inferred flow paths.

Figure 7. Seismic profile 20110419 exhibiting drift deposits in the Agulhas basin directly south of the Agulhas Ridge. The location of the line is shown in Fig. 1b. Vertical exaggeration is ~36.

Figure 8. Inferred bottom current pathways for the time interval ~ 33 ma to present. Found sediment drift deposits are shown as yellowish areas. Darker shading indicates greater sediment thickness. Brown lines indicate mounded drift structures observed in seismic profiles. Red arrows mark LCDW flow around the Agulhas Ridge. Pink arrows indicate the pathway of the returning LCDW around the Cape Rise seamounts. Estimated relative flow intensity is indicated by arrow size. The inset shows a sketch of the suspected early Oligocene to present day LCDW bottom circulation scheme along todays 4900 m depth contour.

References

Alves, T.M., 2010. A 3-D morphometric analysis of erosional features in a contourite drift from offshore SE Brazil. Geophysical Journal International 183, 1151-1164.

Anderson, L.D., Delaney, M.L., 2005. Use of multiproxy records on the Agulhas Ridge, Southern Ocean (Ocean Drilling Project Leg 177, Site 1090) to investigate sub-Antarctic hydrography from the Oligocene to the early Miocene. Paleoceanography 20, PA3011.

Arhan, M., Mercier, H., Park, Y.-H., 2003. On the deep water circulation of the eastern South Atlantic Ocean. Deep-Sea Research Part I-Oceanographic Research Papers 50, 889-916.

Barker, P.F., Diekmann, B., Escutia, C., 2007. Onset of Cenozoic Antarctic glaciation. Deep-Sea Research Part Ii-Topical Studies in Oceanography 54, 2293-2307.

Becker, J.J., Sandwell, D.T., Smith, W.H.F., Braud, J., Binder, B., Depner, J., Fabre, D., Factor, J., Ingalls, S., Kim, S.H., Ladner, R., Marks, K., Nelson, S., Pharaoh, A., Trimmer, R., Von Rosenberg, J., Wallace, G., Weatherall, P., 2009. Global Bathymetry and Elevation Data at 30 Arc Seconds Resolution: SRTM30_PLUS. Marine Geodesy 32, 355-371.

Ben-Avraham, Z., Hartnady, C.J.H., Kitchin, K.A., 1997. Structure and tectonics of the Agulhas-Falkland fracture zone. Tectonophysics 282, 83-98.

Biastoch, A., Boning, C.W., Lutjeharms, J.R.E., 2008. Agulhas leakage dynamics affects decadal variability in Atlantic overturning circulation. Nature 456, 489-492.

Bijl, P.K., Bendle, J.A.P., Bohaty, S.M., Pross, J., Schouten, S., Tauxe, L., Stickley, C.E., McKay, R.M., Röhl, U., Olney, M., Sluijs, A., Escutia, C., Brinkhuis, Expedition 318 Scientists, 2013. Eocene cooling linked to early flow across the Tasmanian Gateway. Proceedings of the National Academy of Sciences 110, 9645-9650.

Billups, K., Channell, J.E.T., Zachos, J., 2002. Late Oligocene to early Miocene geochronology and paleoceanography from the subantarctic South Atlantic. Paleoceanography 17.

Carter, L., McCave, I.N., 1994. Development of sediment drifts approaching an active plate margin under the SW Pacific Deep Western Boundary Current. Paleoceanography 9, 1061-1085.

Carter, R.M., Carter, L., Davy, B., 1994. Seismic stratigraphy of the Bounty Trough, south-west Pacific Ocean. Marine and Petroleum Geology 11, 79-93.

Carter, R.M., McCave, I.N., Carter, L., 2004. Leg 181 Synthesis: Fronts, Flows, Drifts, Volcanoes, and the Evolution of the Southwestern Gateway to the Pacific Ocean, Eastern New Zealand, in: Richter, C. (Ed.), Proc. ODP, Sci. Results 181. Ocean Driling Program, College Station (TX), pp. 1–111.

Charles, C.D., Fairbanks, R.G., 1992. Evidence from Southern Ocean sediments for the effect of North Atlantic deep-water flux on climate. Nature 355, 416-419.

Dencausse, G., Arhan, M., Speich, S., 2010. Routes of Agulhas rings in the southeastern Cape Basin. Deep-Sea Research Part I-Oceanographic Research Papers 57, 1406-1421.

Diekmann, B., Kuhn, G., Gersonde, R., Mackensen, A., 2004. Middle Eocene to early Miocene environmental changes in the sub-Antarctic Southern Ocean: evidence from biogenic and terrigenous depositional patterns at ODP Site 1090. Global and Planetary Change 40, 295-313.

Eagles, G., Livermore, R., Morris, P., 2006. Small basins in the Scotia Sea: The Eocene Drake Passage gateway. Earth and Planetary Science Letters 242, 343-353.

Ehrmann, W.U., Mackensen, A., 1992. Sedimentological evidence for the formation of an East Antarctic ice sheet in Eocene/Oligocene time. Palaeogeography, Palaeoclimatology, Palaeoecology 93, 85-112.

Escutia, C., Nelson, C.H., Acton, G.D., Eittreim, S.L., Cooper, A.K., Warnke, D.A., Jaramillo, J.M., 2002. Current controlled deposition on the Wilkes Land continental rise, Antarctica, in: Stow, D.A.V., Pudsey, C.J., Howe, J.A., Faugeres, J.C., Viana, A. (Eds.), Contourite Systems: Modern drifts and Ancient Series, seismic and Sedimentary Characteristics. Geological Society, London, Memoir, pp. 373-384.

Faugères, J.-C., Stow, D.A.V., Imbert, P., Viana, A., 1999. Seismic features diagnostic of contourite drifts. Marine Geology 162, 1-38.

Faugères, J.C., Stow, D.A.V., 2008. Contourite Drifts: Nature, Evolution and Controls, in: Rebesco, M., Camerlenghi, A. (Eds.), Contourites. Elsevier, pp. 257-288.

Flood, R.D., 1988. A lee wave model for deep-sea mudwave activity. Deep Sea Research Part A. Oceanographic Research Papers 35, 973-983.

Gersonde, R., Hodell, D.A., Blum, P., Andersson, C., Austin, W.E.N., Billups, K., Channell, J.E.T., Charles, C.D., Diekmann, B., Filippelli, G.M., Flores, J.A., Hewitt, A.T., Howard, W.R., Ikehara, M., Janecek, T.R., Kanfoush, S.L., Kemp, A.E.S., King, S.L., Kleiven, H.F., Kuhn, G., Marino, M., Ninnemann, U.S., O'Connell, S., Ortiz, J.D., Stoner, J.S., Sugiyama, K., Warnke, D.A., Zielinski, U., 1999. Leg 177 summary; Southern Ocean Paleoceanography. Proc. ODP, Init. Repts., 177. Ocean Drilling Program, College Station, TX pp. 1-67.

Gruetzner, J., Uenzelmann-Neben, G., Franke, D., 2012. Variations in sediment transport at the central Argentine continental margin during the Cenozoic. Geochemistry Geophysics Geosystems 13, Q10003.

Hailwood, E., Clement, B., 1991. Magnetostratigraphy of Sites 703 and 704, Meteor Rise, Southeastern South Atlantic, in: Ciesielski, P.F., Kristoffersen, Y. et al. (Eds.), Proceedings of the Ocean Drilling Program: Scientific results. Ocean Drilling Program, College Station, TX, pp. 367-386.

Hartnady, C.J.H., Leroex, A.P., 1985. Southern-Ocean Hotspot Tracks and the Cenozoic Absolute Motion of the African, Antarctic, and South-American Plates. Earth and Planetary Science Letters 75, 245-257.

Hernández-Molina, F.J., Llave, E., Stow, D.A.V., 2008a. Continental Slope Contourites, in: Rebesco, M., Camerlenghi, A. (Eds.), Contourites. Elsevier, Amsterdam, pp. 379-408.

Hernández-Molina, F.J., Maldonado, A., Stow, D.A.V., 2008b. Abyssal Plain Contourites, in: Rebesco, M., Camerlenghi, A. (Eds.), Contourites. Elsevier, pp. 345-378.

Hernández-Molina, F.J., Paterlini, M., Violante, R., Marshall, P., de Isasi, M., Somoza, L., Rebesco, M., 2009. Contourite depositional system on the Argentine Slope: An exceptional record of the influence of Antarctic water masses. Geology 37, 507-510.

Hinz, K., Neben, S., Schreckenberger, B., Roeser, H.A., Block, M., Souza, K.G.d., Meyer, H., 1999. The Argentine continental margin north of 48°S: sedimentary successions, volcanic activity during breakup. Marine and Petroleum Geology 16, 1-25.

Hodell, D.A., Gersonde, R., Blum, P., 2002. Leg 177 synthesis: insights into Southern Ocean paleoceanography on tectonic to millennial timescales, in: Hodell, D.A., Gersonde, R., Blum, P. (Eds.), Proc. ODP, Sci. Results, 177, pp. 1-54.

Horn, M., Uenzelmann-Neben, G., 2015. The Deep Western Boundary Current at the Bounty Trough, east of New Zealand: Indications for its activity already before the opening of the Tasmanian Gateway. Marine Geology 362, 60-75.

Katz, M.E., Cramer, B.S., Toggweiler, J.R., Esmay, G., Liu, C., Miller, K.G., Rosenthal, Y., Wade, B.S., Wright, J.D., 2011. Impact of Antarctic Circumpolar Current Development on Late Paleogene Ocean Structure. Science 332, 1076-1079.

Latimer, J.C., Filippelli, G.M., 2002. Eocene to Miocene terrigenous inputs and export production: geochemical evidence from ODP Leg 177, Site 1090. Palaeogeography Palaeoclimatology Palaeoecology 182, 151-164.

le Roex, A., Class, C., O'Connor, J., Jokat, W., 2010. Shona and Discovery Aseismic Ridge Systems, South Atlantic: Trace Element Evidence for Enriched Mantle Sources. Journal of Petrology 51, 2089-2120.

Maldonado, A., Barnolas, A., Bohoyo, F., Escutia, C., Galindo-Zaldívar, J., Hernández-Molina, J., Jabaloy, A., Lobo, F.J., Nelson, C.H., Rodríguez-Fernández, J., Somoza, L., Vázquez, J.-T., 2005. Miocene to Recent contourite drifts development in the northern Weddell Sea (Antarctica). Global and Planetary Change 45, 99-129.

Marino, M., Flores, J.A., 2002. Miocene to Pliocene calcareous nannofossil biostratigraphy at ODP Leg 177 Sites 1088 and 1090. Marine Micropaleontology 45, 291-307.

Masson, D.G., Bett, B.J., Billett, D.S.M., Jacobs, C.L., Wheeler, A.J., Wynn, R.B., 2003. The origin of deep-water, coral-topped mounds in the northern Rockall Trough, Northeast Atlantic. Marine Geology 194, 159-180.

Masson, D.G., Howe, J.A., Stoker, M.S., 2002. Bottom-current sediment waves, sediment drifts and contourites in the northern Rockall Trough. Marine Geology 192, 215-237.

McCave, I.N., Hall, I.R., 2006. Size sorting in marine muds: Processes, pitfalls, and prospects for paleoflow-speed proxies. Geochemistry Geophysics Geosystems 7, Q10N05.

Merrifield, M.A., Holloway, P.E., Johnston, T.M.S., 2001. The generation of internal tides at the Hawaiian Ridge. Geophysical Research Letters 28, 559-562.

Müller-Michaelis, A., Uenzelmann-Neben, G., Stein, R., 2013. A revised Early Miocene age for the instigation of the Eirik Drift, offshore southern Greenland: Evidence from high-resolution seismic reflection data. Marine Geology 340, 1-15.

Munday, D.R., Johnson, H.L., Marshall, D.P., 2015. The role of ocean gateways in the dynamics and sensitivity to wind stress of the early Antarctic Circumpolar Current. Paleoceanography 30, 284-302.

Muñoz, A., Cristobo, J., Rios, P., Druet, M., Polonio, V., Uchupi, E., Acosta, J., 2012. Sediment drifts and cold-water coral reefs in the Patagonian upper and middle continental slope. Marine and Petroleum Geology 36, 70-82.

Nelson, C.H., Baraza, J., Maldonado, A., Rodero, J., Escutia, C., Barber, J.H., 1999. Influence of the Atlantic inflow and Mediterranean outflow currents on Late Quaternary sedimentary facies of the Gulf of Cadiz continental margin. Marine Geology 155, 99-129.

Nielsen, T., Knutz, P.C., Kuijpers, A., 2008. Seismic Expression of Contourite Depositional Systems, in: Rebesco, M., Camerlenghi, A. (Eds.), Contourites. Elsevier, pp. 301-321.

Niemi, T.M., Ben-Avraham, Z., Hartnady, C.J.H., Reznikov, M., 2000. Post-Eocene seismic stratigraphy of the deep ocean basin adjacent to the southeast African continental margin: a record of geostrophic bottom current systems. Marine Geology 162, 237-258.

Pena, L.D., Goldstein, S.L., 2014. Thermohaline circulation crisis and impacts during the mid-Pleistocene transition. Science 345, 318-322.

Rebesco, M., Camerlenghi, A., 2008. Contourites, in: van Loon, A.J. (Ed.), Developments in Sedimentology. Elsevier, Amsterdam, p. 688.

Rebesco, M., Hernández-Molina, F.J., Van Rooij, D., Wåhlin, A., 2014. Contourites and associated sediments controlled by deep-water circulation processes: State-of-the-art and future considerations. Marine Geology 352, 111-154.

Scher, H.D., Martin, E.E., 2006. Timing and Climatic Consequences of the Opening of Drake Passage. Science 312, 428-430.

Scher, H.D., Martin, E.E., 2008. Oligocene deep water export from the North Atlantic and the development of the Antarctic Circumpolar Current examined with neodymium isotopes. Paleoceanography 23, PA1205.

Scher, H.D., Whittaker, J.M., Williams, S.E., Latimer, J.C., Kordesch, W.E.C., Delaney, M.L., 2015. Onset of Antarctic Circumpolar Current 30 million years ago as Tasmanian Gateway aligned with westerlies. Nature 523, 580-583.

Shannon, L.V., Hunter, D., 1988. Notes on Antarctic Intermediate Water around Southern-Africa. South African Journal of Marine Science 6, 107-117.

Shipboard Scientific Party, 1999. Site 1090, in: Gersonde, R., Hodell, D.A., Blum, P. et al. (Eds.), Proceedings of the Ocean Drilling Program: Initial Reports 177. Ocean Drilling Program, College Station, TX, pp. 1–101.

Sijp, W.P., England, M.H., Huber, M., 2011. Effect of the deepening of the Tasman Gateway on the global ocean. Paleoceanography 26, PA4207, doi:10.1029/2011PA002143..

Stichel, T., Frank, M., Rickli, J., Haley, B.A., 2012. The hafnium and neodymium isotope composition of seawater in the Atlantic sector of the Southern Ocean. Earth and Planetary Science Letters 317–318, 282-294.

Stow, D.A.V., Faugeres, J.-C., Howe, J.A., Pudsey, C.J., Viana, A.R., 2002. Bottom currents, contourites and deep-sea sediment drifts; current state-of-the-art, in: Stow, D.A.V., Faugeres, J.-C., Howe, J.A., Pudsey, C.J., Viana, A.R. (Eds.), Deep-water contourite systems; modern drifts and ancient series, seismic and sedimentary characteristics. Geological Society of London Memoirs, London, pp. 7-20.

Stow, D.A.V., Faugères, J.C., 2008. Contourite Facies and the Facies Model in: Rebesco, M., Camerlenghi, A. (Eds.), Contourites. Elsevier, Amsterdam, pp. 223-256.

Stow, D.A.V., Hernandez-Molina, F.J., Llave, E., Sayago-Gil, M., del Rio, V.D., Branson, A., 2009. Bedform-velocity matrix: The estimation of bottom current velocity from bedform observations. Geology 37, 327-330.

Tucholke, B.E., Embley, R.W., 1984. Cenozoic regional erosion of the abyssal sea floor off South Africa, in: Schlee, J.S. (Ed.), Interregional Unconformities and Hydrocarbon Accumulation. AAPG Memoir, pp. 145-164.

Uenzelmann-Neben, G., 2001. Seismic characteristics of sediment drifts: An example from the Agulhas Plateau, southwest Indian Ocean. Marine Geophysical Researches 22, 323-343.

Uenzelmann-Neben, G., 2012. The expedition of the research vessel "Maria S. Merian" to the South Atlantic in 2011 (MSM 19/2). Alfred Wegener Institute for Polar and Marine Research, Bremerhaven.

Uenzelmann-Neben, G., Gohl, K., 2004. The Agulhas Ridge, South Atlantic: The peculiar structure of a fracture zone. Marine Geophysical Researches 25, 305-319.

Uenzelmann-Neben, G., Schlüter, P., Weigelt, E., 2007. Cenozoic oceanic circulation within the South African gateway: indications from seismic stratigraphy. South African Journal of Geology 110, 275-294.

van Sebille, E., Johns, W.E., Beal, L.M., 2012. Does the vorticity flux from Agulhas rings control the zonal pathway of NADW across the South Atlantic? Journal of Geophysical Research: Oceans 117, C05037.

Wåhlin, A.K., Cenedese, C., 2006. How entraining density currents influence the stratification in a one-dimensional ocean basin. Deep Sea Research Part II: Topical Studies in Oceanography 53, 172-193.

Wildeboer Schut, E., Uenzelmann-Neben, G., 2005. Cenozoic bottom current sedimentation in the Cape basin, South Atlantic. Geophysical Journal International 161, 325-333.

Wildeboer Schut, E., Uenzelmann-Neben, G., 2006. Tying seismic data to geologic information from core data: an example from ODP Leg 177. Geo-Marine Letters 26, 235-248.

Wildeboer Schut, E., Uenzelmann-Neben, G., Gersonde, R., 2002. Seismic evidence for bottom current activity at the Agulhas Ridge. Global and Planetary Change 34, 185-198.

Zachos, J., Pagani, M., Sloan, L., Thomas, E., Billups, K., 2001. Trends, Rhythms, and Aberrations in Global Climate 65 Ma to Present. Science 292, 686-693.

Figure 1

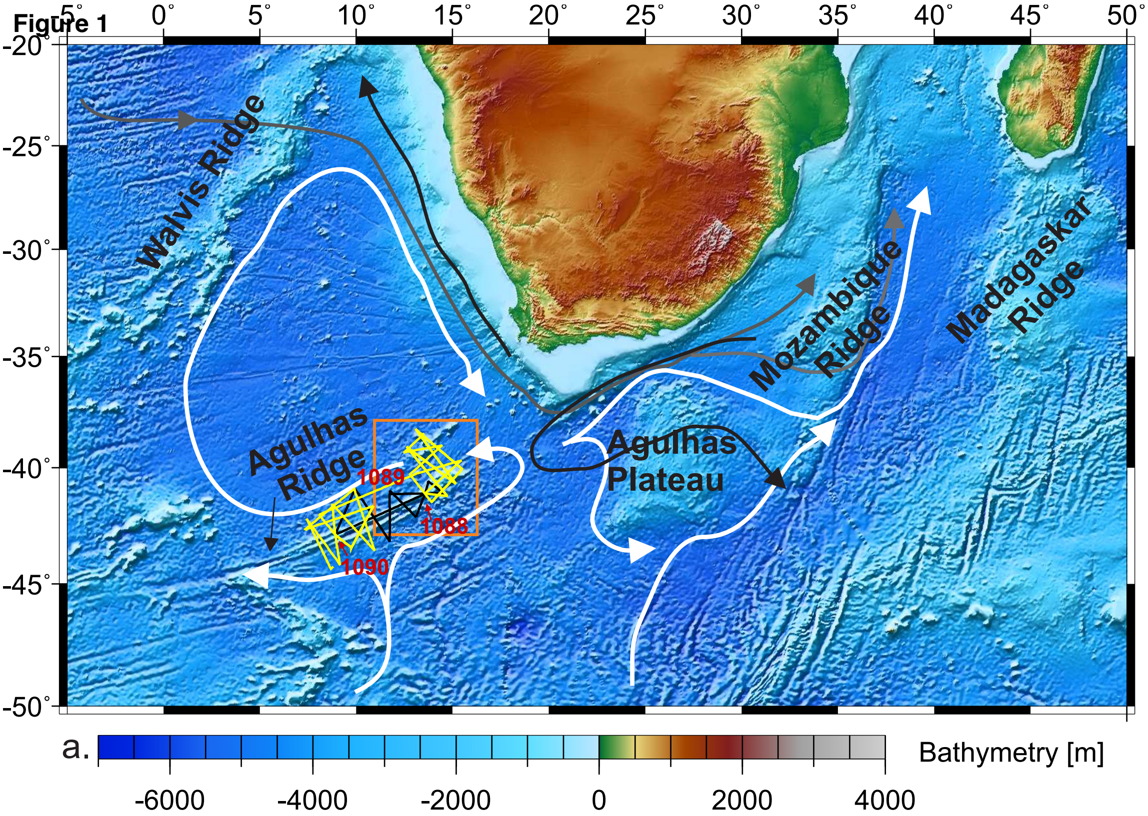

Walvis Ridge
Agulhas Ridge
1089
1088
1090
Agulhas Plateau
Mozambique Ridge
Madagaskar Ridge
a.
Bathymetry [m]

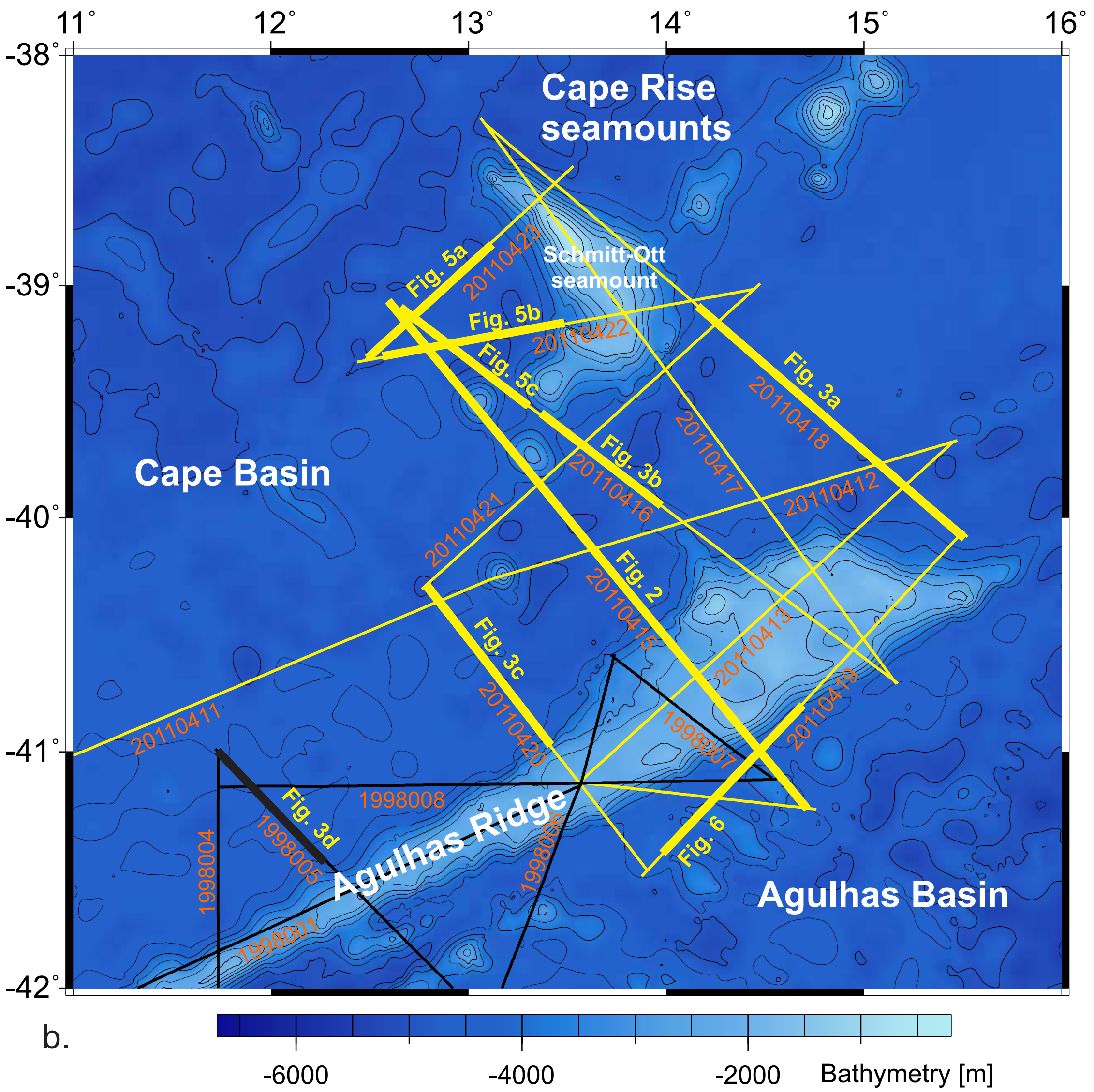

Cape Rise seamounts
Schmitt-Ott seamount
Cape Basin
Agulhas Ridge
Agulhas Basin
Fig. 5a
Fig. 5b
Fig. 5c
Fig. 3a
Fig. 3b
Fig. 3c
Fig. 3d
Fig. 2
Fig. 6
20110423
20110422
20110418
20110417
20110416
20110421
20110415
20110412
20110413
20110419
20110420
20110411
1998008
1998007
1998004
1998005
1998006
1998001
b.
Bathymetry [m]

Figure 2

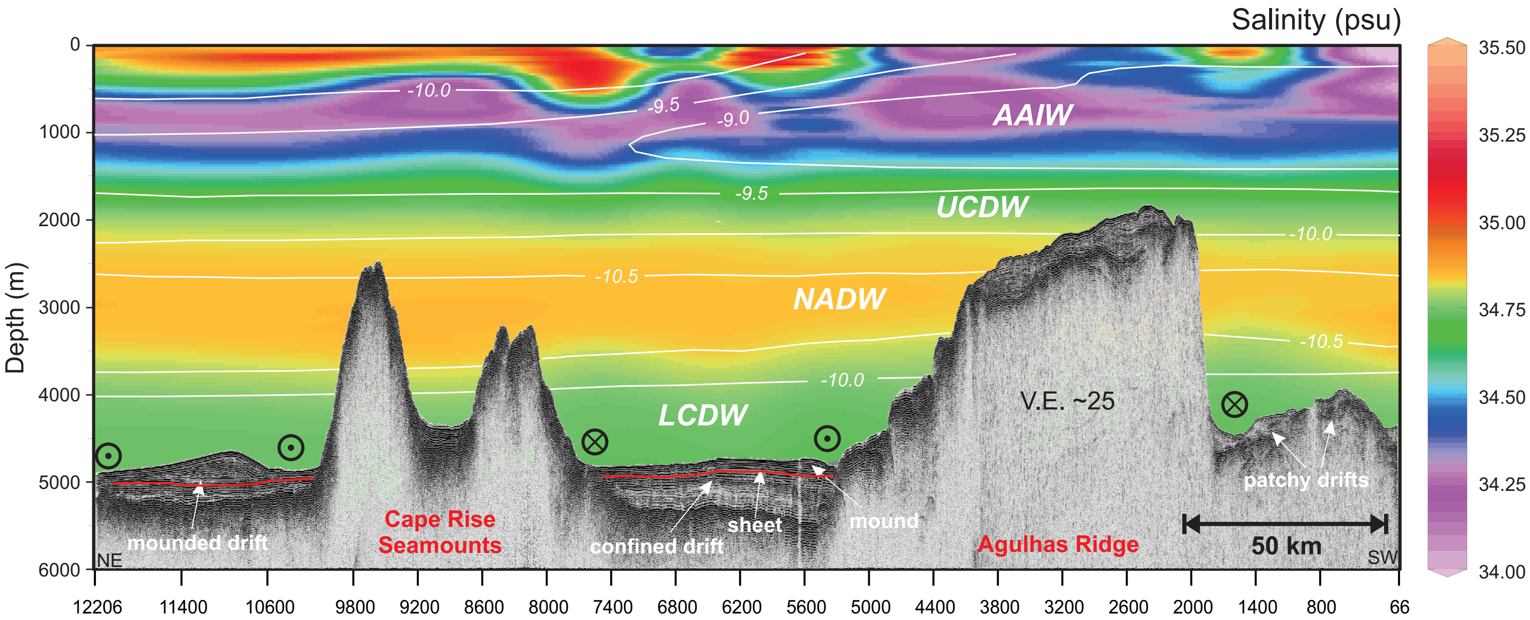

Salinity (psu)
35.50
35.25
35.00
34.75
34.50
34.25
34.00
Depth (m)
0
1000
2000
3000
4000
5000
6000
12206
11400
10600
9800
9200
8600
8000
7400
6800
6200
5600
5000
4400
3800
3200
2600
2000
1400
800
66
-10.0
-9.5
-9.0
AAIW
-9.5
UCDW
-10.0
-10.5
NADW
-10.5
-10.0
LCDW
V.E. ~25
mounded drift
Cape Rise
Seamounts
confined drift
sheet
mound
Agulhas Ridge
patchy drifts
50 km
NE
SW

Figure 3

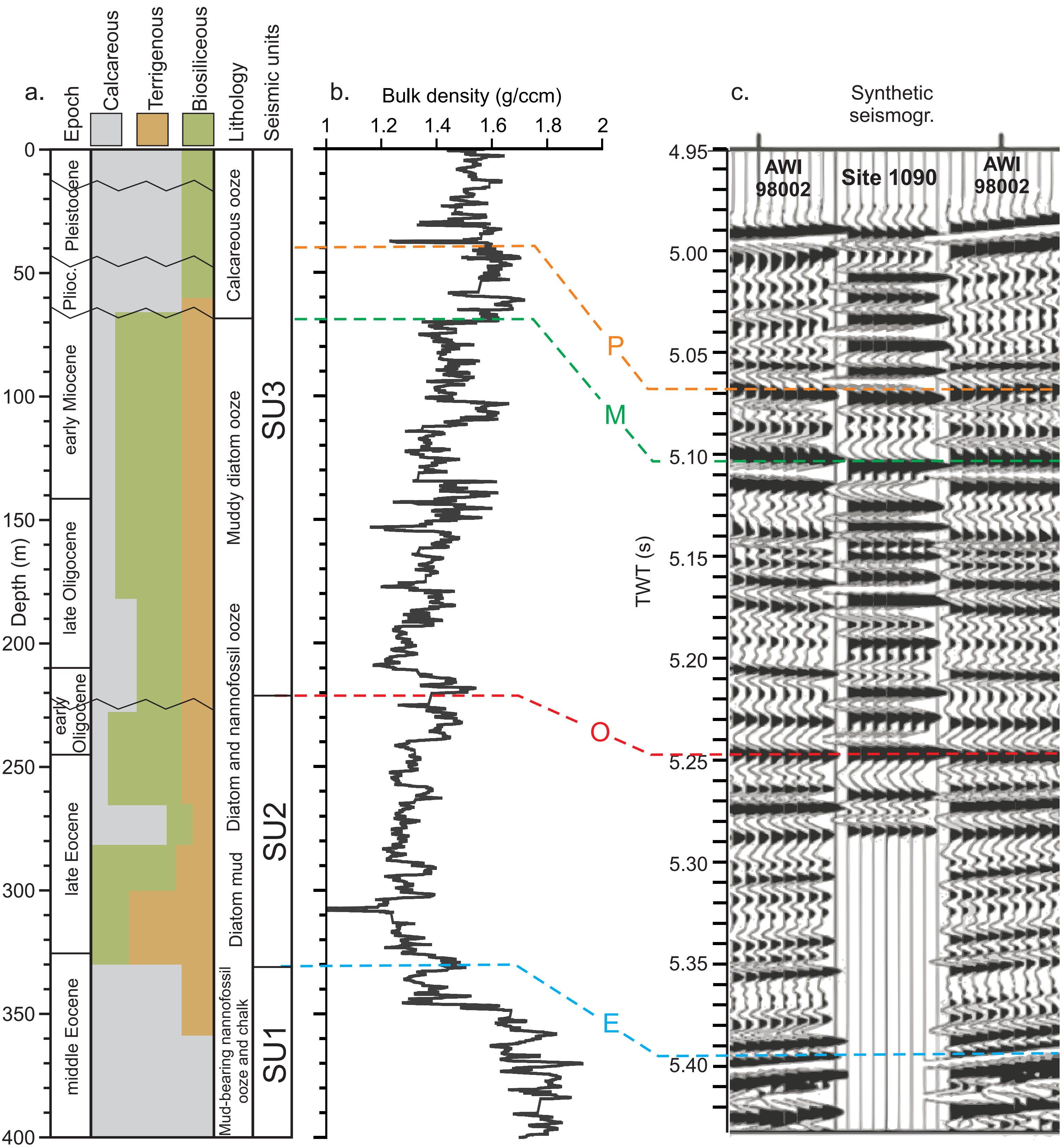

a.
Epoch
Calcareous
Terrigenous
Biosiliceous
Lithology
Seismic units
Depth (m)
0
50
100
150
200
250
300
350
400
Pleistocene
Plioc.
early Miocene
late Oligocene
early Oligocene
late Eocene
middle Eocene
Calcareous ooze
Muddy diatom ooze
Diatom and nannofossil ooze
Diatom mud
Mud-bearing nannofossil ooze and chalk
SU3
SU2
SU1
b.
Bulk density (g/ccm)
1
1.2
1.4
1.6
1.8
2
P
M
O
E
c.
Synthetic seismogr.
AWI 98002
Site 1090
AWI 98002
TWT (s)
4.95
5.00
5.05
5.10
5.15
5.20
5.25
5.30
5.35
5.40

Figure 4

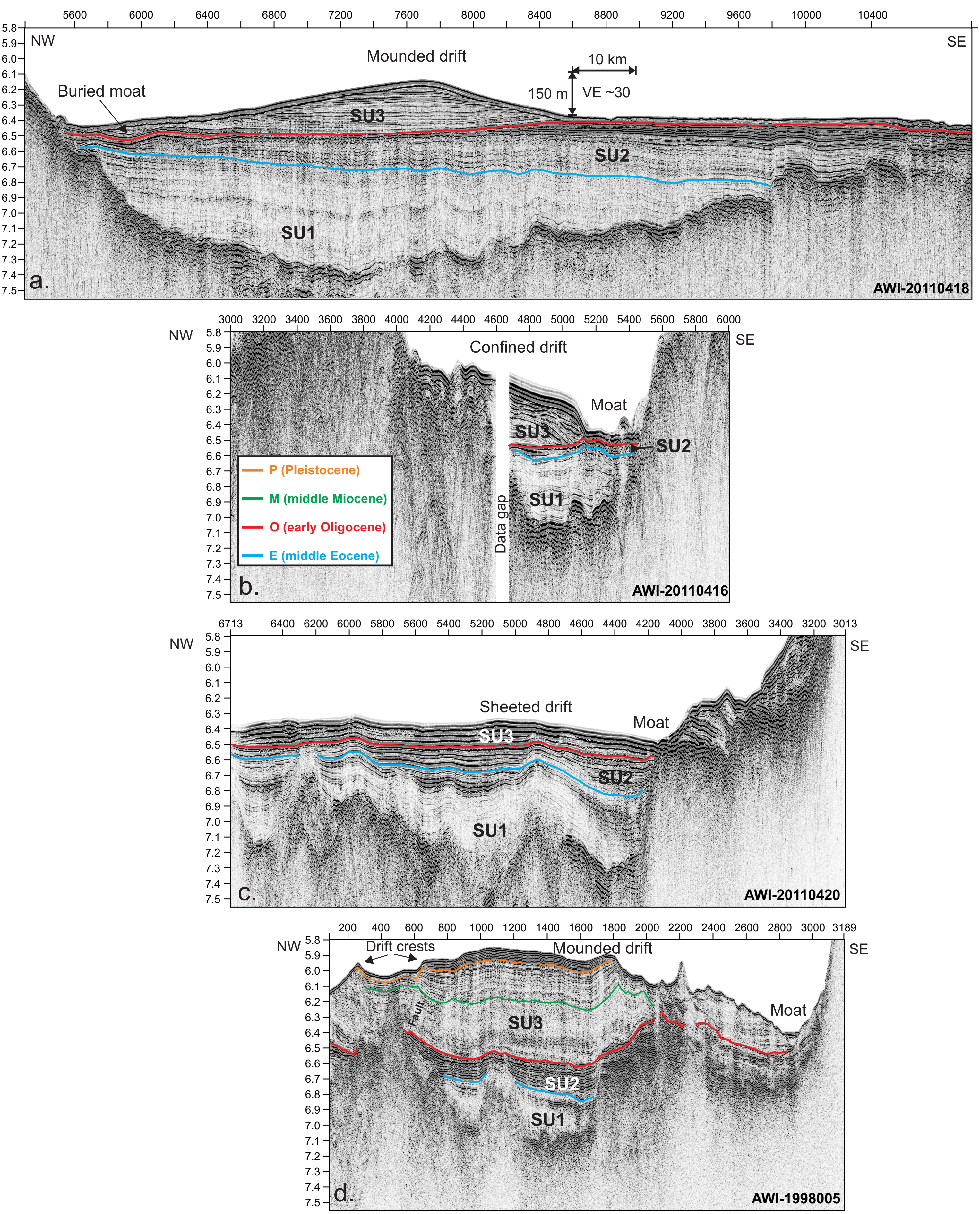

NW
SE
Mounded drift
Buried moat
10 km
150 m
VE ~30
SU3
SU2
SU1
a.
AWI-20110418
Confined drift
Moat
Data gap
P (Pleistocene)
M (middle Miocene)
O (early Oligocene)
E (middle Eocene)
b.
AWI-20110416
Sheeted drift
c.
AWI-20110420
Drift crests
Fault
d.
AWI-1998005

Figure 5

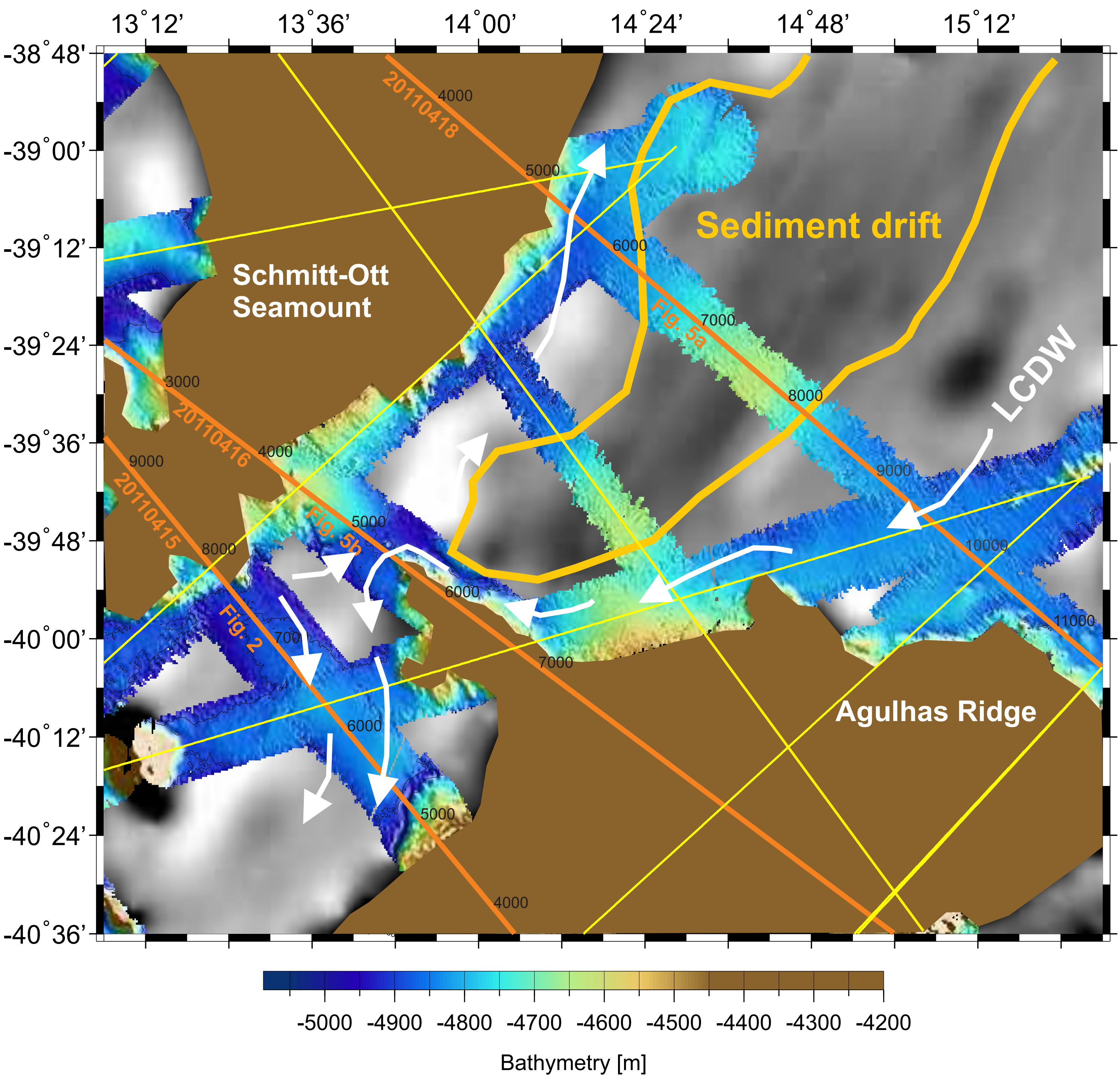

13˚12'
13˚36'
14˚00'
14˚24'
14˚48'
15˚12'
-38˚48'
-39˚00'
-39˚12'
-39˚24'
-39˚36'
-39˚48'
-40˚00'
-40˚12'
-40˚24'
-40˚36'
Sediment drift
Schmitt-Ott Seamount
LCDW
Agulhas Ridge
20110418
20110416
20110415
Fig. 5a
Fig. 5b
Fig. 2
-5000
-4900
-4800
-4700
-4600
-4500
-4400
-4300
-4200
Bathymetry [m]

Figure 6

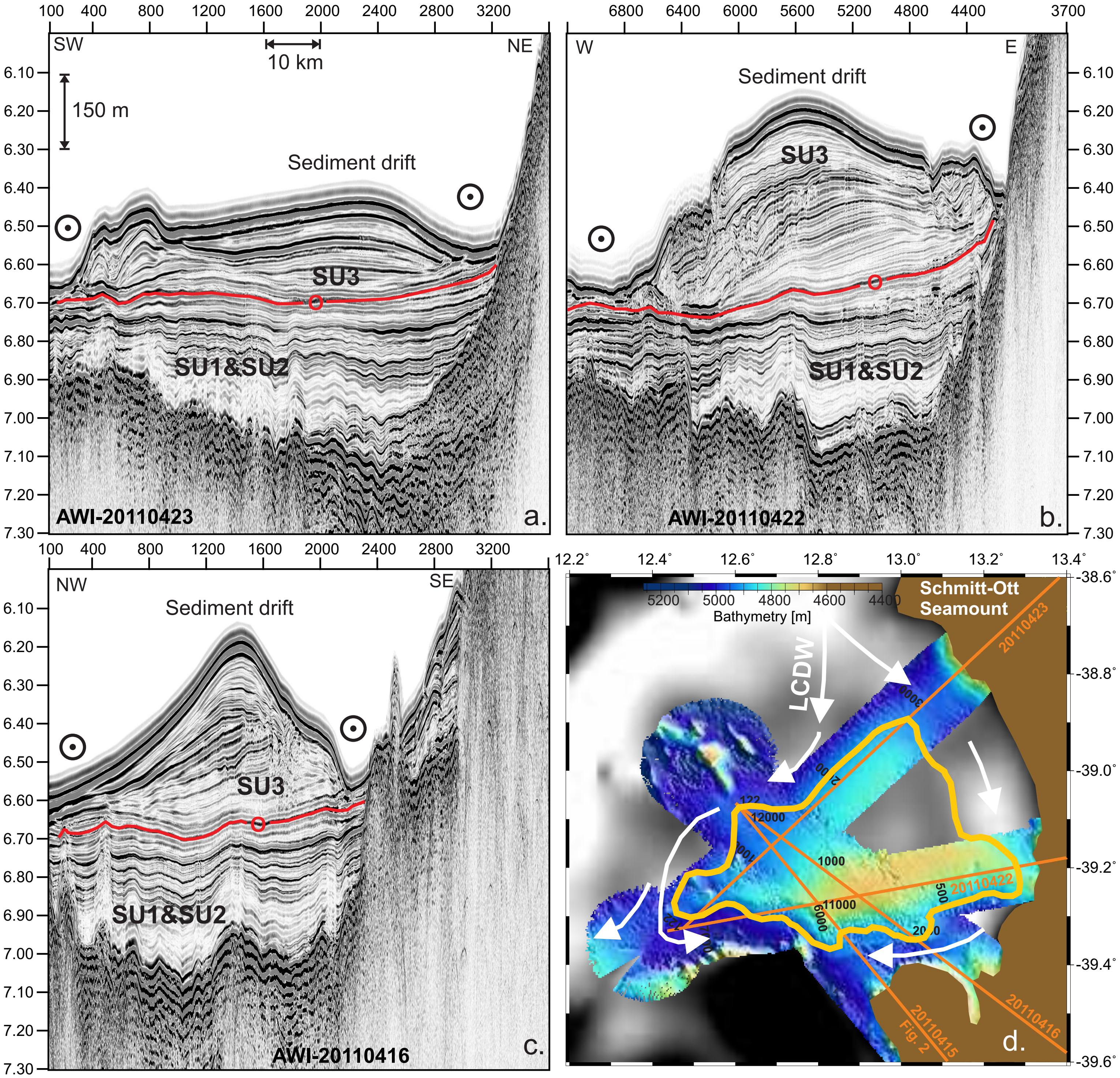

SW
NE
10 km
150 m
Sediment drift
SU3
SU1&SU2
AWI-20110423
a.
W
E
Sediment drift
SU3
SU1&SU2
AWI-20110422
b.
NW
SE
Sediment drift
SU3
SU1&SU2
AWI-20110416
c.
Schmitt-Ott Seamount
Bathymetry [m]
5200 5000 4800 4600 4400
LCDW
20110423
20110422
20110416
20110415
Fig. 2
d.

Figure 7

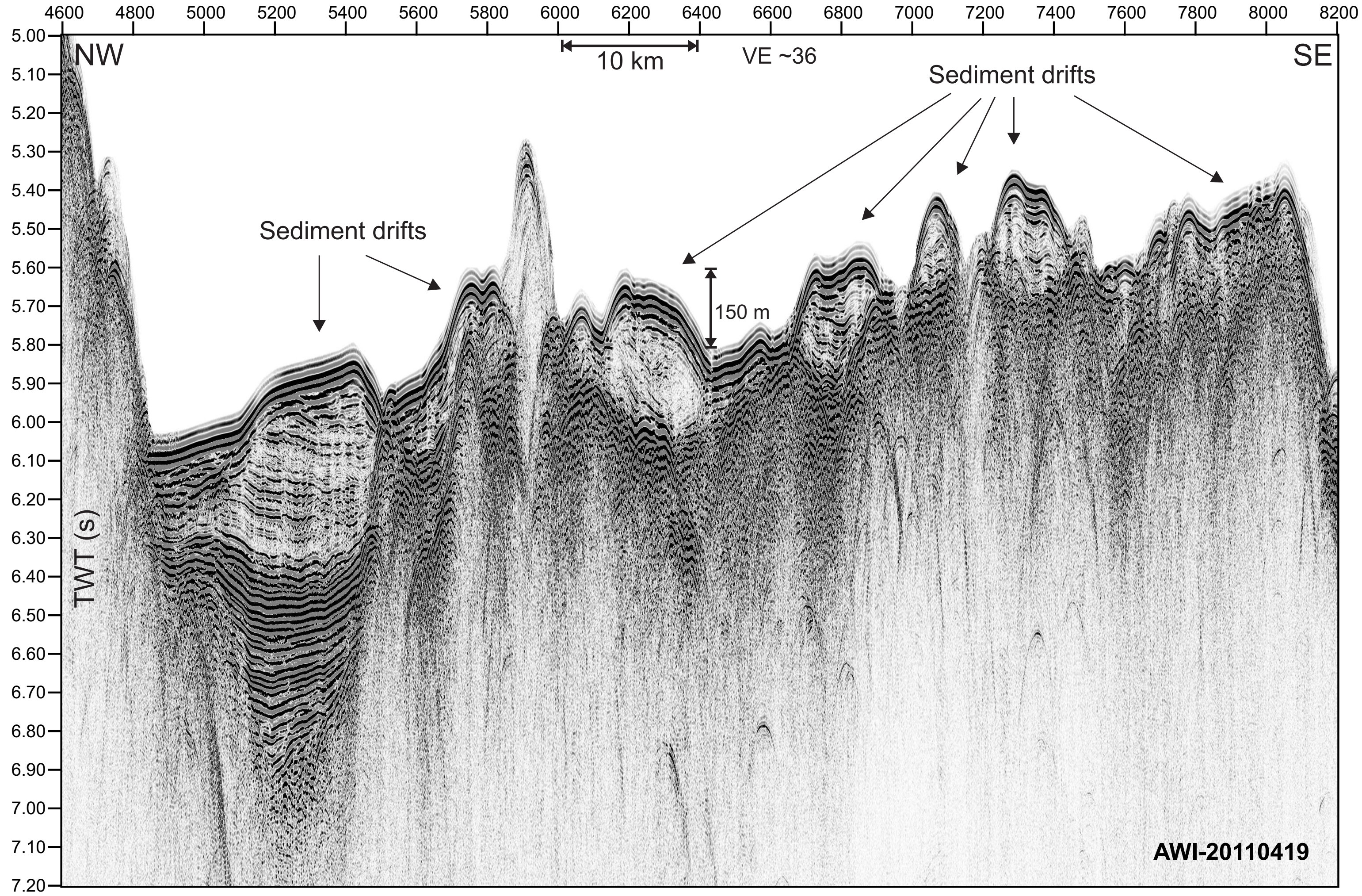
4600
4800
5000
5200
5400
5600
5800
6000
6200
6400
6600
6800
7000
7200
7400
7600
7800
8000
8200
5.00
5.10
5.20
5.30
5.40
5.50
5.60
5.70
5.80
5.90
6.00
6.10
6.20
6.30
6.40
6.50
6.60
6.70
6.80
6.90
7.00
7.10
7.20
NW
10 km
VE ~36
SE
Sediment drifts
Sediment drifts
150 m
TWT (s)
AWI-20110419

Figure 8

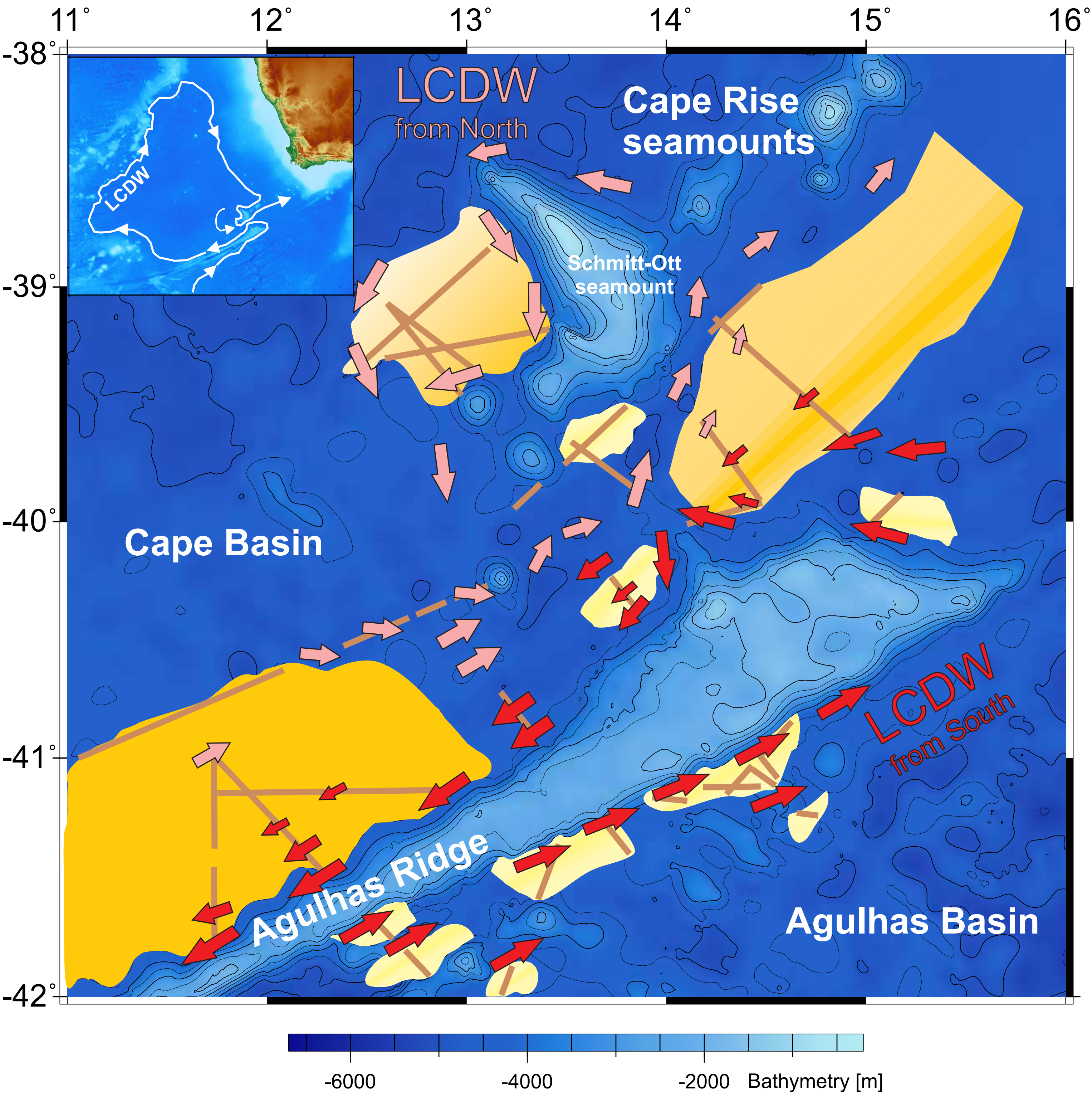
11°
12°
13°
14°
15°
16°
-38°
-39°
-40°
-41°
-42°
LCDW
LCDW
from North
Cape Rise
seamounts
Schmitt-Ott
seamount
Cape Basin
Agulhas Ridge
LCDW
from South
Agulhas Basin
-6000
-4000
-2000
Bathymetry [m]